*Nanochem Res 9(2): 153-161, Spring 2024*

RESEARCH PAPER

# Neodymium-doped SnS nanomaterials: ultrasound-assisted synthesis, characterization, and investigation of its physical properties

***Mostafa Yousefi, Younes Hanifehpour*, Mehdi Abdolmaleki, Negin Rahmani***

*Department of Chemistry, Sayyed Jamaleddin Asadabadi University, Asadabad, Iran*

**ARTICLE INFO**

***Article History:***
*Received 23 January 2024*
*Accepted 12 March 2024*
*Published 15 April 2024*

***Keywords:***
*Tin sulfide*
*Neodymium*
*Ultrasound-assisted*
*Bandgap*
*4-probe*
*Diffuse reflectance spectroscopy*

**ABSTRACT**

In this research, tin sulfide compounds and their dope in different percentages with neodymium were prepared by the sonochemical method. Next, the surface and structure of the synthesized samples were thoroughly analyzed using different detection techniques such as scanning electron microscopy, X-ray energy scattering, X-ray photoelectron spectroscopy, and X-ray diffraction. The X-ray diffraction pattern showed that the crystalline phase of tin sulfide and its doping with neodymium was orthorhombic and the results of elemental analysis confirmed the presence of tin, sulfur, and neodymium elements. Based on SEM images, the morphology of the prepared SnS was crystalline and changed to a nanoflower structure after Nd doping. After examining the surface morphology and structure of the synthesized samples, diffuse reflectance spectroscopy (DRS) and 4-probe techniques were employed to study the optical properties and electrical conductivity of these compounds. Band gap calculations based on absorption spectrum data indicated that the band gap decreased with the increase in dopant amount. Additionally, with the increase in the amount of dopant and temperature, the electrical resistance declined and the electrical conductivity increased.

**How to cite this article**
*Yousefi M., Hanifehpour Y., Abdolmaleki M., Rahmani N. Neodymium-doped SnS nanomaterials: ultrasound-assisted synthesis, characterization, and investigation of its physical properties. Nanochem Res, 2024; 9(2):153-161. DOI: 10.22036/ncr.2024.02.007*

## INTRODUCTION

Sonochemistry or the use of ultrasound waves is one of the effective methods to perform chemical reactions in recent years for the synthesis of nanostructure materials. The basis for the creation of this technique is based on a process called cavitation, which creates a very high local temperature and pressure in the reaction environment. This process includes the creation, gradual growth, and finally the explosion of a series of bubbles due to the application of ultrasonic waves to the solution, which produces a shock wave. The energy from this wave is used to break covalent bonds, homogenize, and perform some chemical shock reactions, especially the synthesis of nanoparticles, synthesis of organic substances, etc. [1-3]. Cavitation-induced sonochemistry provides a unique interaction between energy and matter, with hot spots inside the bubbles of ~5000 K, pressures of ~1000 bar, heating and cooling rates of $>10^{10}$ K $s^{-1}$; these extraordinary conditions permit access to a range of chemical reaction space normally not accessible, which allows for the synthesis of a wide variety of unusual nanostructured materials [4-6].

The process that occurs due to the application of ultrasound waves to the solution, including the formation, growth and bursting of bubbles in the liquid, is known. The growth of the bubble is through penetration and the solvent vapor enters the bubble under the name of cavitation and continues until the bubble bursts. The bursting of the bubble causes the release of energy locally and

* Corresponding Author Email: *Hanifehpour@sjau.ac.ir*

makes it possible to carry out a chemical reaction. The principles of the theory of local release of energy due to cavitation are investigated using the hot spot theory, and based on this theory, a very high local temperature is created as a result of the explosion of bubbles in the solution. The efficiency of sonochemical reactions is directly dependent on the energy caused by the cavitation process, which itself depends on various factors such as the frequency used, the intensity of the waves used, the temperature of the environment, the type of solvent, the pressure applied to the system, etc. By carefully controlling these parameters and optimizing the conditions, various chemical reactions, especially the synthesis of various nanoparticles, can be performed in the best way and with high efficiency [7-12].

Tin sulfide, which is a member of group IV-VI metal chalconides, has attracted attention due to its narrow bandwidth and appropriate optical and electronic properties. There are three types of crystal structure including orthorhombic, high zinc and distorted salt structure for tin sulfide; however, the structure of most tin sulfide films is orthorhombic. Its direct optical bandwidth was in the range of 1.5-1.2 ev and the indirect bandwidth was between 1-1.2 ev. The conductivity of tin sulfide is high and it is of p type. At temperatures above 265 degrees Celsius, SnS slowly decomposes into 2SnS and tin. 2SnS has a bandwidth of 2.07 ev and its conductivity is of n type [13-15].

Tin sulfide is a layered semiconductor that is promising for converting solar photoelectrochemical energy into electrical energy due to its very high conductivity. This composition is made of tin (member of group 4) and sulfur (member of group 6). According to Hoffmann's studies, tin sulfide has an orthorhombic structure, which can also be described as pseudotetragonal.

In general, luminescent materials consist of a host lattice, which is doped with small amounts of photoluminescent ions, and the host increases or decreases the luminescence property of the doped material. Most of the luminescent materials are oxides, sulfides and their doped types with cations of intermediate or lanthanide elements [16-18]. Lanthanide cations with empty 5d orbitals and partly occupied 4f orbitals could also mainly enhance the separation rate of photo-induced charge carriers within semiconductor catalysts and improve significantly the catalytic activity [19, 20].

Lanthanide ions have good fluorescence due to their stability and high emission quantum efficiency. If these cations can be doped inside the semiconductor, excitation of the energy gap of the semiconductor leads to energy transfer to these cations, causing an increase in their luminescence emission [21-25].

Since the optical, magnetic and electrical properties of lanthanide cations are highly important, the doping effect of these cations in tin chalcogenide structures can also be highly important and create new applications for these materials. Therefore, the aim of this research work is the synthesis of tin sulfide nanocrystals doped with neodymium cation by sonochemical method and investigation of the effect of various factors on the morphology of the synthesized compounds. Since the substitution of metal ions with different radii instead of $Sn^{2+}$ causes a change in the electrical conductivity of these compounds, their optical and conductive properties will also be investigated.

## EXPERIMENTAL

### *Materials And Methods*

All chemicals utilized in this research were of analytical grade and were used without further purification. $SnCl_2$ and thioacetamide were obtained from Merck. $Nd(NO_3)_3.6H_2O$ and ethanol (99%) were purchased from Aldrich.

### *Ultrasound-assisted synthesis of SnS and $Nd^{3+}$-doped SnS nanomaterials*

In a routine preparation, 1.89 grams of tin chloride and 0.76 grams of thioacetamide were added to 50 ml of deionized water and the mixture was stirred for 30 minutes under a temperature of 50 °C with a magnetic stirrer. Subsequently, the reaction mixture was transferred to the ultrasonic bath and placed in it at a temperature of 50 °C for 3 hours. Finally, upon cooling down at room temperature, due to the fineness of the particles and passing through the filter paper, the resulting colloid was subject to centrifugation with distilled water and alcohol. This process yielded a black powdery precipitate. The sediment was placed in a thermal oven at a temperature of 60°C for 24 hours to dry. The resulting black powder was used to continue the testing and analysis process. The method of preparing SnS doped compounds with various content of neodymium was the same as the pure SnS synthesis method. Only the amount of tin chloride was reduced and the amount of $Nd(NO_3)_3$ was increased based on stoichiometic calculations.

*Characterization Methods*

The XRPD characterization was employed for the determination of samples' crystal phase composition at room temperature via a D8 advance diffractometer (Bruker, Karlsruhe, Germany) with high-intensity monochromatic Cu K*a* radiation (λ=1.5406 A˚), accelerating voltage of 40 kV and an emission current of 30 mA. Elemental analyses were carried out using a linked ISIS300, Oxford EDS (energy dispersion spectroscopy) detector. Utilizing an electron microscope (SEM, S-4200, Hitachi, Tokyo, Japan), the surface state and the morphology were observed. The assessment of the chemical state of the constituent elements and chemical identification were conducted using X-ray photoelectron spectroscopy, XPS (K-ALPHA, UK) Thermo Scientific spectrophotometer. The DRS spectra of the as-prepared compounds were recorded by HO-SP-DRS 100. The electrical resistivity of the compounds was measured through the 4-point probe technique.

## RESULTS AND DISCUSSION

*Physical properties and characteristics of as-prepared materials*

Fig. 1 and 2 indicate the XRD pattern of pure SnS prepared by the sonochemical route. These patterns demonstrate that in the above concentration of the doping agent (neodymium), the orthorhombic crystal phase related to the structure of tin sulfide is preserved and no impurity peak can be seen up to 10% concentration of doping in the corresponding pattern. It is also in full compliance with the standard card (card no. JCPDS-89-0253), and the crystal lattice constants are a = 11.312 Å, b = 3.971 Å, c = 4.305 Å [26, 27]. By increasing the doping concentration to higher percentages, the impurity peaks are seen next to the peaks related to tin sulfide, which indicates that neodymium ions are not placed in the tin sites in the structure.

SEM analysis was carried out to investigate the morphologies of the products. Fig. 3a displays the SEM image of pure SnS, revealing a nanocrystalline structure in its morphology. By incorporating $Nd^{3+}$ ions into the lattice of SnS, the size and surface morphology of the sample indicate clear changes. By doping of neodymium, the uniform nanoflowers were observed in the 10% Nd-doped SnS sample (Fig. 3a, 3b).

XPS analysis was applied to investigate the chemical composition and the valence state of Nd in the 10% $Nd^{3+}$-doped SnS particles (Fig.s 4-6). The Sn $3d_{1/2}$ and $3d_{3/2}$ peaks are noted at around 486.1 eV and 494.2 eV which can be attributed

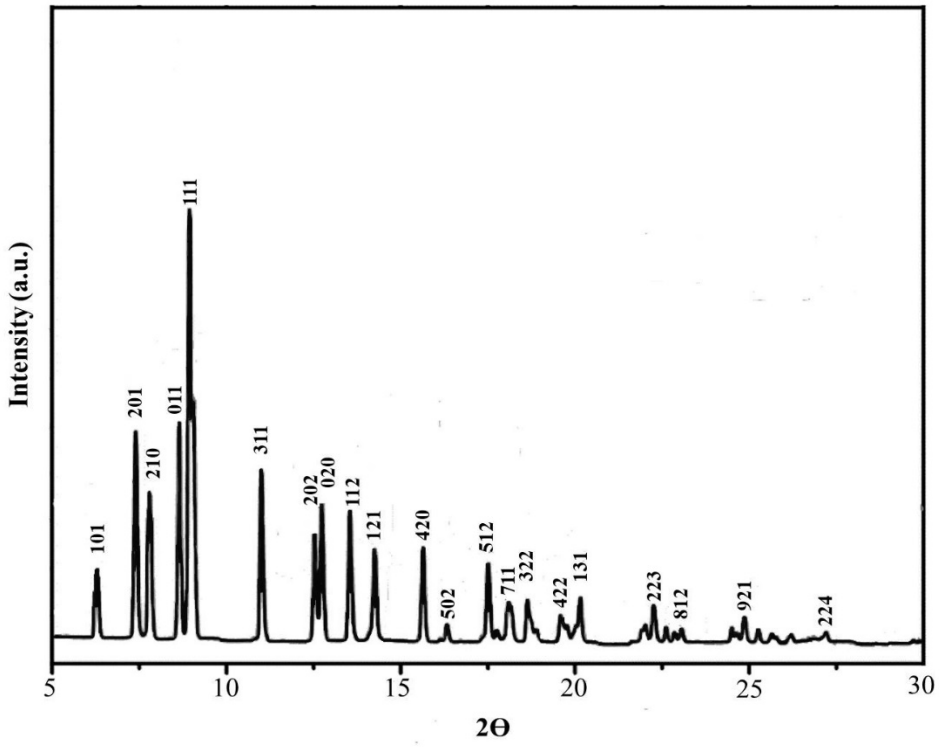


Fig. 1. The XRD pattern of pure SnS synthesized through the sonochemical method.

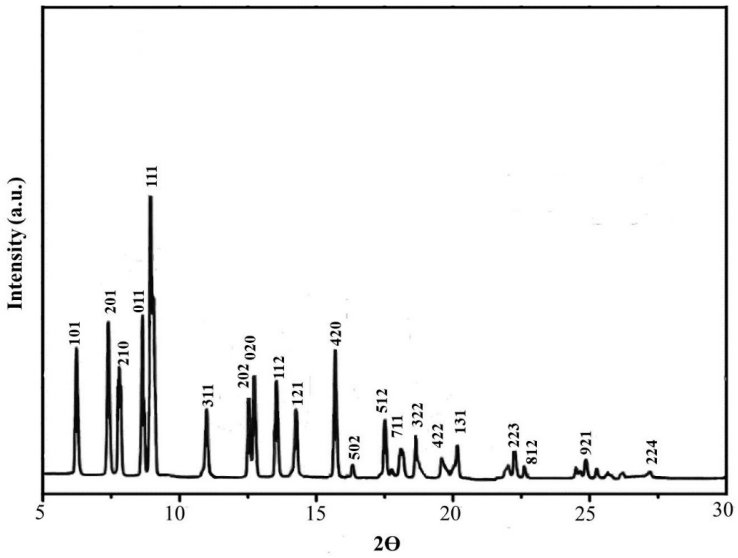


Fig. 2. The XRD pattern of 10% Nd-doped SnS synthesized through the sonochemical method.

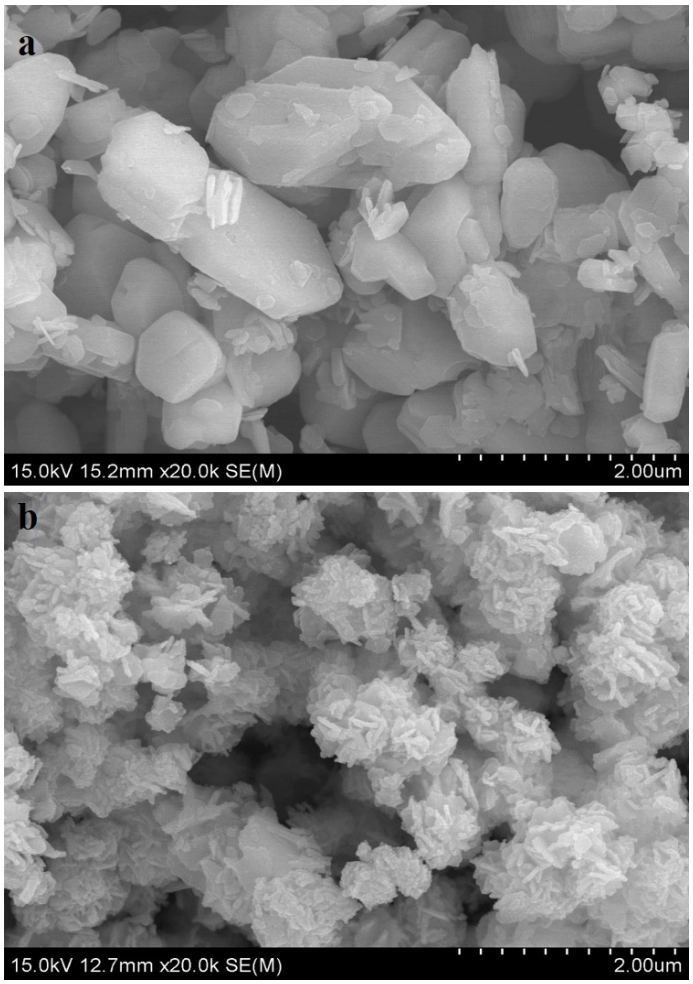


Fig. 3. SEM images of (a) nanocrystalline pure SnS and (b) 10 % Nd-doped SnS nanoflowers.

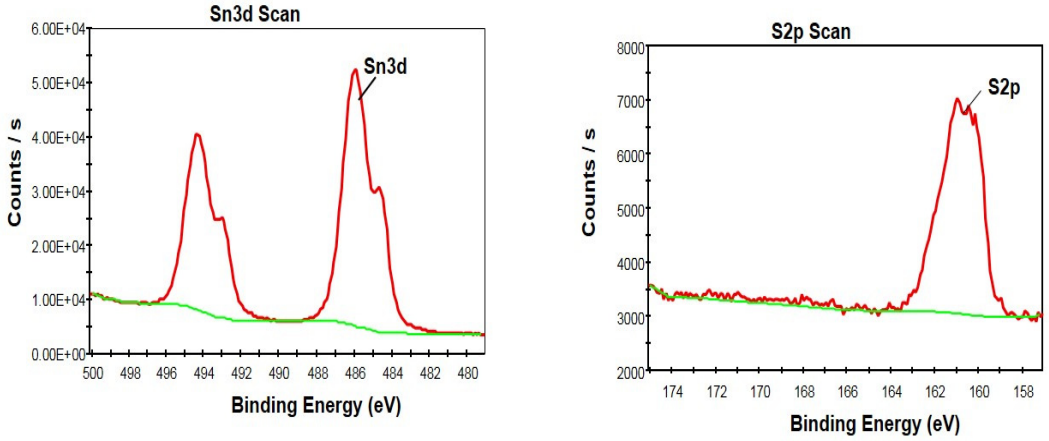


Fig. 4. The XPS spectra of pure SnS synthesized through the sonochemical method.

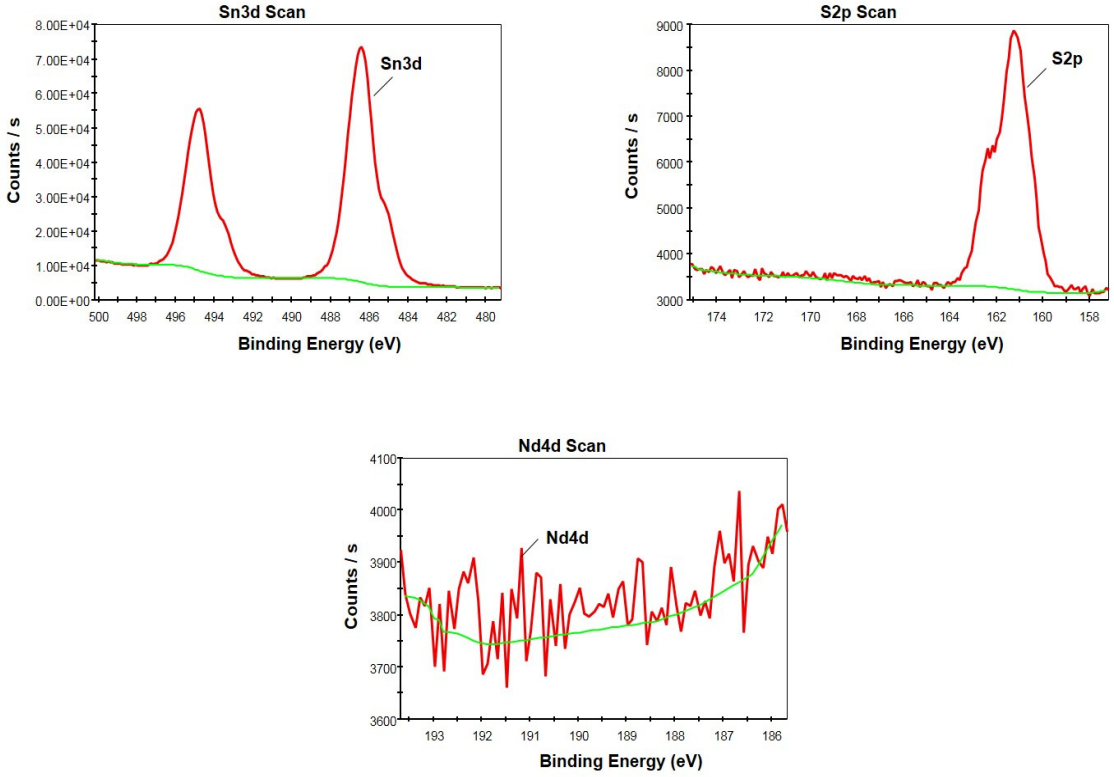


Fig. 5. The XPS spectra of 6% Nd-doped SnS synthesized through the sonochemical method.

to the Sn element in tin sulfide and validates the oxidation state of 2 for Sn in the 10 % $Nd^{3+}$-doped SnS sample [28]. The S2p curve of SnS displays a strong peak at around 161.8 eV, which is attributed to the coordination of Sulfur and Sn atoms (Sn–S–Sn) in the structure of SnS [29]. As seen in the XPS figures, the peak centered at 191.2 eV can be attributed to the Nd 4d.

A diffuse reflectance spectrometer (DRS) was employed to study the optical properties of tin sulfide compounds doped with neodymium. Fig. 7 shows the absorption spectrum of tin sulfide. The DRS spectra of various Nd-doped compounds are provided in the supplementary data as S1.

To calculate the band gap of the prepared compounds, Tauc's equation was used. Therefore, by increasing the amount of dopant, the amount of band gap decreases, and this reduction of band

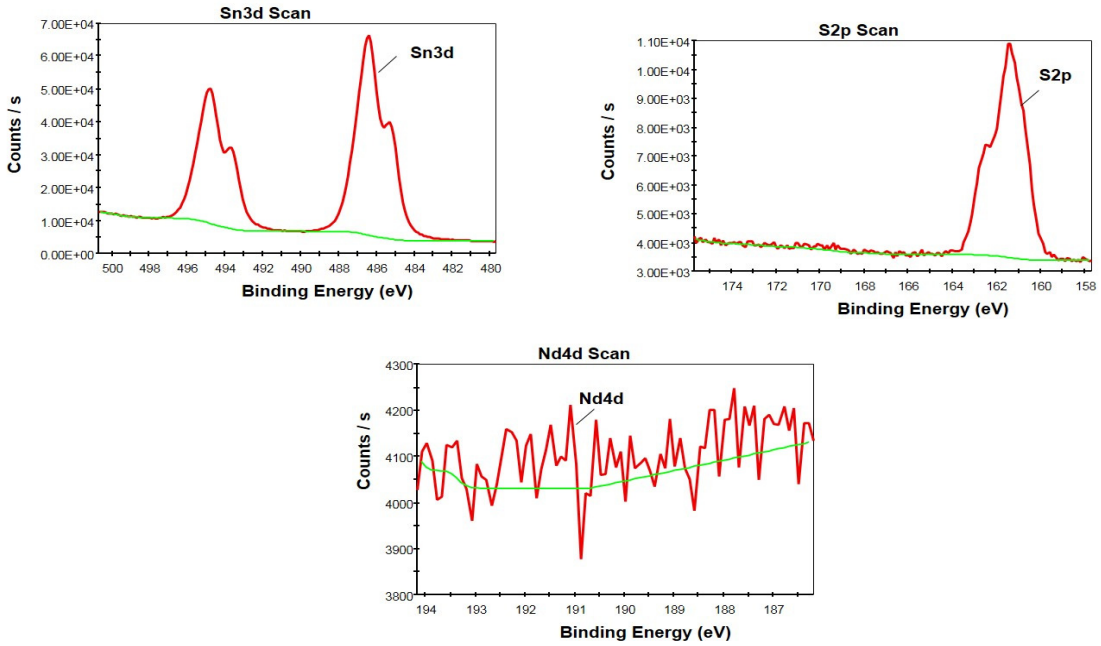


Fig. 6. The XPS spectra of 10% Nd-doped SnS synthesized through the sonochemical method.

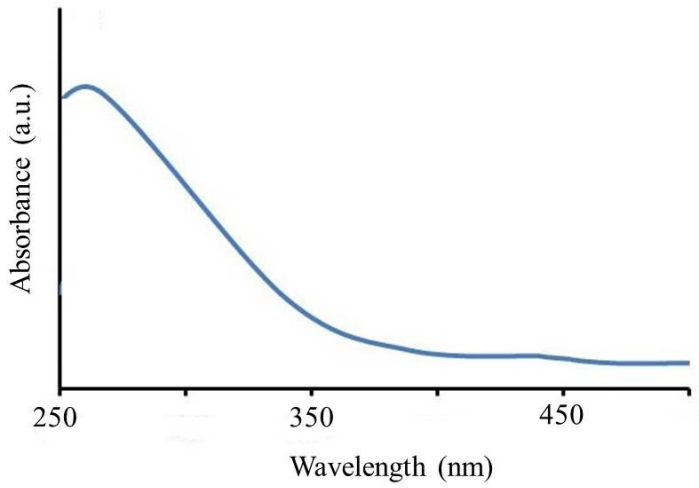


Fig. 7. DRS spectra of pure SnS.

gap can play an important role in increasing the efficiency of their semiconductor and photocatalytic properties. Fig. 8 displays the Tauc plot of $Sn_{1-x}Nd_xS$ nanomaterials.

The electrical resistivity of the compounds is shown in Fig. 9. With the increase in the neodymium cation concentration, the electrical resistivity of synthesized nanomaterials decreased obviously. At room temperature the electrical resistivity of pure SnS was of the order of 0.0897 Ω.m, while for $Sn_{0.9}Nd_{0.1}S$ it was 0.0887 Ω.m, respectively. Electrical resistivity decreases linearly with temperature.

The temperature dependence of the electrical resistivity for $Sn_{0.9}Nd_{0.1}S$ between 290-340K is shown in Fig. 10. As a result, the electrical conductance of Nd-doped SnS materials is higher than pure tin sulfide at room temperature and increases with temperature.

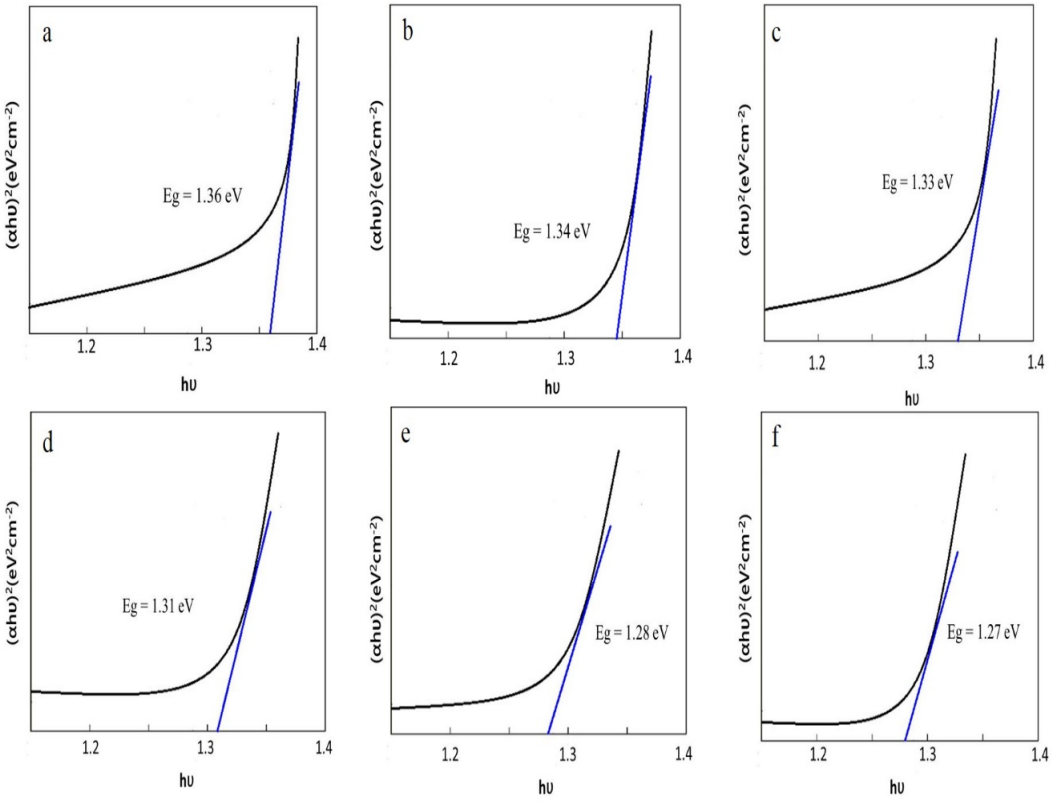


Fig. 8. Calculation of bandgap based on Tauc plots.

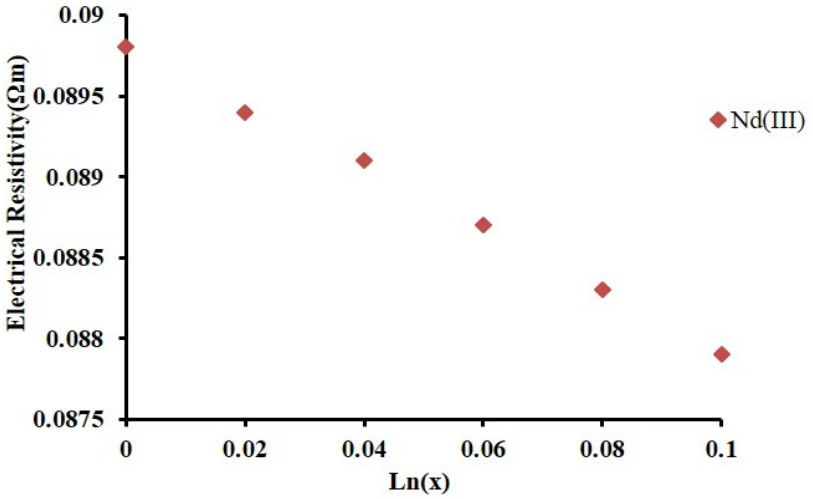


Fig. 9. The electrical resistivity of as-prepared Nd-doped SnS compounds.

## CONCLUSION

In this study, both pure and $Nd^{3+}$–doped SnS were obtained by a simple sonochemical approach. The XRD analysis displayed a well acrystalline orthorhombic structure of SnS. The substitution of $Nd^{3+}$ions into the SnS lattice was validated by the EDX and XPS analyses. The surface morphology and size of the samples had no obvious changes after incorporating $Nd^{3+}$ into the lattice of SnS. The bandgap of as-prepared compounds was calculated via the Tauc equation and showed linear dependence between electrical resistivity

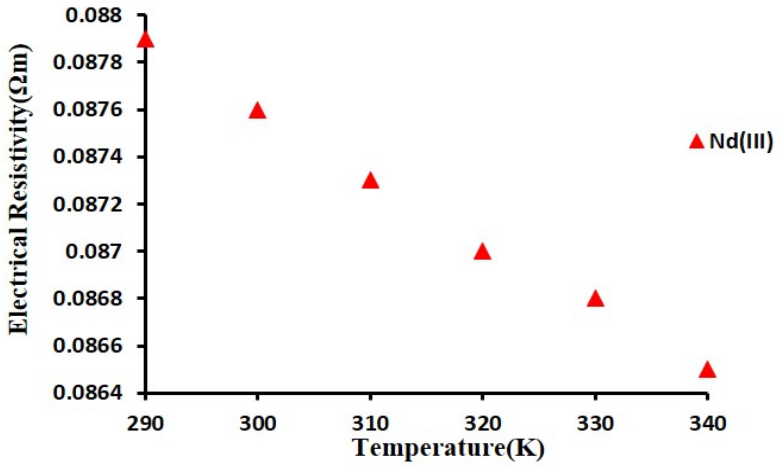


Fig. 10. Temperature dependent of the electrical resistivity of as-prepared Nd-doped SnS compounds.

and dopant contents. The electrical conductance of Nd-doped SnS materials was higher than pure tin sulfide at room temperature and increased with temperature. Consequently, the ultrasound method is a low cost, reliable and eco-friendly route for the preparation of Nd-doped SnS nanoparticles and the obtained compounds can be employed for supercapacitor application and enhanced photocatalyst due to their modified bandgap.

## ACKNOWLEDGMENT

This work is funded by Sayyed Jamaleddin Asadabadi University Research Grant.

## CONFLICTS OF INTEREST

The authors declare that there are no conflicts of interest regarding the publication of this paper.

## REFERENCES

1. Melikhov IV. Crystallization behavior of nanodisperse phases. Inorganic Materials. 2000;36(3):278-86.
2. Sergeev GB. Nanochemistry: Elsevier; 2006.
3. Gedanken A. Using sonochemistry for the fabrication of nanomaterials. Ultrasonics Sonochemistry. 2004;11(2):47-55.
4. Bang JH, Suslick KS. Applications of Ultrasound to the Synthesis of Nanostructured Materials. Advanced Materials. 2010;22(10):1039-59.
5. parhizkar J, Habibi MH. Synthesis, characterization and photocatalytic properties of Iron oxide nanoparticles synthesized by sol-gel autocombustion with ultrasonic irradiation. Nanochemistry Research. 2017;2(2):166-71.
6. Shahbazi-Alavi H, Safaei-Ghomi J. Nano-Fe3O4 attached to Crosslinked sulfonated polyacrylamide (Cross-PAA-SO3H) as high performance catalyst for the synthesis of thiazoles under ultrasonic irradiations. Nanochemistry Research. 2019;4(1):55-63.
7. Bhangu SK, Ashokkumar M. Theory of Sonochemistry. In: Colmenares JC, Chatel G, editors. Sonochemistry: From Basic Principles to Innovative Applications. Cham: Springer International Publishing; 2017. p. 1-28.
8. Thompson LH, Doraiswamy LK. Sonochemistry: Science and Engineering. Industrial & Engineering Chemistry Research. 1999;38(4):1215-49.
9. Chatel G. Sonochemistry: new opportunities for green chemistry: World Scientific Publishing Company; 2016.
10. Ley SV, Low CM. Ultrasound in synthesis: Springer Science & Business Media; 2012.
11. Boldyrev VV. Mechanochemistry and sonochemistry. Ultrasonics Sonochemistry. 1995;2(2):S143-S5.
12. Li Z, Dong J, Zhang H, Zhang Y, Wang H, Cui X, et al. Sonochemical catalysis as a unique strategy for the fabrication of nano-/micro-structured inorganics. Nanoscale Advances. 2021;3(1):41-72.
13. Zhang H, Hu C, Wang X, Xi Y, Li X. Synthesis and photosensitivity of SnS nanobelts. Journal of Alloys and Compounds. 2012;513:1-5.
14. Ray SC, Karanjai MK, DasGupta D. Structure and photoconductive properties of dip-deposited SnS and SnS2 thin films and their conversion to tin dioxide by annealing in air. Thin Solid Films. 1999;350(1):72-8.
15. Akkari A, Guasch C, Kamoun-Turki N. Chemically deposited tin sulphide. Journal of Alloys and Compounds. 2010;490(1):180-3.
16. Liu X, Wang X. Preparation and luminescence properties of BaZrO3:Eu phosphor powders. Optical Materials. 2007;30(4):626-9.
17. Qiu J, Miura K, Sugimoto N, Hirao K. Preparation and fluorescence properties of fluoroaluminate glasses containing Eu2+ ions. Journal of Non-Crystalline Solids. 1997;213-214:266-70.
18. Hamnabard N, Hanifehpour Y, Khomami B, Woo Joo S. Synthesis, characterization and photocatalytic performance of Yb-doped CdTe nanoparticles. Materials Letters. 2015;145:253-7.
19. Hanifehpour Y. Co-Reduction synthesis and Characterization of Ytterbium-substituted ZnS Nanoparticles and Investigation of Catalytic Performance. Nanochemistry Research. 2021;6(2):202-12.

20. Hanifehpour Y, Soltani B, Amani-Ghadim AR, Hedayati B, Khomami B, Joo SW. Synthesis and characterization of samarium-doped ZnS nanoparticles: A novel visible light responsive photocatalyst. Materials Research Bulletin. 2016;76:411-21.
21. Hanifehpour Y, Woo Joo S. Synthesis, characterization and sonophotocatalytic degradation of an azo dye on Europium doped cadmium selenide nanoparticles. Nanochemistry Research. 2018;3(2):178-88.
22. Alemi A, Hanifehpour Y, Woo Joo S, Khandar A, Morsali A, Min B-K. Co-reduction synthesis of new LnxSb2−xS3 (Ln: Nd3+, Lu3+, Ho3+) nanomaterials and investigation of their physical properties. Physica B: Condensed Matter. 2011;406(14):2801-6.
23. Khataee A, Darvishi Cheshmeh Soltani R, Hanifehpour Y, Safarpour M, Gholipour Ranjbar H, Joo SW. Synthesis and Characterization of Dysprosium-Doped ZnO Nanoparticles for Photocatalysis of a Textile Dye under Visible Light Irradiation. Industrial & Engineering Chemistry Research. 2014;53(5):1924-32.
24. Alemi A, Hanifehpour Y, Joo SW, Min B-K. Synthesis of novel LnxSb2−xSe3 (Ln: Lu3+, Ho3+, Nd3+) nanomaterials via co-reduction method and investigation of their physical properties. Colloids and Surfaces A: Physicochemical and Engineering Aspects. 2011;390(1):142-8.
25. Khataee A, Khataee A, Fathinia M, Hanifehpour Y, Joo SW. Kinetics and Mechanism of Enhanced Photocatalytic Activity under Visible Light Using Synthesized PrxCd1–xSe Nanoparticles. Industrial & Engineering Chemistry Research. 2013;52(37):13357-69.
26. Gawai U, Gaikwad D, Patil S, Pandey K, Lalla N, Dole B. Synthesis, local structure and optical property studies of α-SnS microrods by synchrotron X-ray pair distribution function and micro-Raman shift. RSC advances. 2020;10(36):21277-82.
27. Salwa AS, Salem A. Linear and nonlinear optical properties of SnS thermally evaporated thin films. Optik. 2019;196:163140.
28. Ravuri S, Pandey CA, Ramchandran R, Jeon SK, Grace AN. Wet Chemical Synthesis of SnS/Graphene Nanocomposites for High Performance Supercapacitor Electrodes. International Journal of Nanoscience. 2017;17(01n02):1760022.
29. Durn JDG, Guindo MC, Delgado AV. Electrophoretic Properties of Colloidal Dispersions of Monodisperse Zinc Sulfide: Effects of Potential-Determining Ions and Surface Oxidation. Journal of Colloid and Interface Science. 1995;173(2):436-42.